Attitude Manoeuvring Under Dynamic Path and Time Constraints for Formation Flying Nanosatellites

B. Johnston-Lemke
University of Toronto Institute for Aerospace Studies Space Flight Laboratory
4925 Dufferin Street, Toronto, Ontario, Canada M3H 5T6**;** +1-416-667-7993
bjlemke@sfl-utias.net

R. E. Zee
University of Toronto Institute for Aerospace Studies Space Flight Laboratory
4925 Dufferin Street, Toronto, Ontario, Canada M3H 5T6**;** +1-416-667-7864
rzee@sfl-utias.net

ABSTRACT

Large angle attitude manoeuvres are often subjected to dynamic and celestial path constraints such as maintaining ground link communication, GPS lock, or Sun avoidance while tracking various primary targets in real time. Considered in this paper is an onboard approach to maximizing the signal lock with GPS satellites with a restricted antenna field of view while tracking primary attitude targets. The proposed time optimal attitude controller does not require a priori knowledge of the target(s) and avoids the time and computational requirements of typical avoidance and random search techniques. Included in this paper are the attitude requirements to maintain GPS lock as derived from ground based and on orbit experiments as well as the proposed controller and the results of numerical simulations. This controller has been developed for the Canadian Advanced Nanosatellite eXperiment (CanX) 4 and 5 satellites currently under development at the University of Toronto's Space Flight Laboratory. CanX-4 and CanX-5 are identical satellites that will be launched together and will make use of differential GPS measurements and a cold gas propulsion system to demonstrate autonomous sub-meter control formation flying based on differential GPS measurements.

INTRODUCTION

Global Positioning System (GPS) aided navigation for Low Earth Orbit (LEO) spacecraft is a demonstrated and growing practice. GPS receivers can be used in LEO for absolute positioning, such as the PROBA-2 [1] or TerraSAR-X [2] missions or for relative navigation, such as CanX-4 and CanX-5, JC2Sat-FF [3] and TanDEM-X [4] formation flying missions. The use of commercial GPS receivers in LEO however is still fraught with challenges. The unique challenge of the LEO environment over ground based commercial receivers is the comparatively larger relative velocities between the receiver's antenna and the GPS satellites. This can lead to lengthy time to first lock, as the receiver needs to search a wide band of Doppler shift when undergoing a cold or warm start [5,6,7]. Once a full position and velocity solution has been computed by the receiver, and an up-to-date almanac is available, the receiver is capable of making reasonable estimates of the Doppler shift and is better able to acquire a lock on further GPS satellites [8]. During an attitude slew, GPS satellites that are being tracked by the receiver will move out of view of the antenna. Similarly, new GPS satellites move into the antenna's field of view. However, these new satellites will not be tracked by the receiver instantaneously. If the time required to acquire these new GPS satellites is sufficiently long compared to the slew rate, GPS satellites will continue to drop out faster than they can be reacquired, resulting in insufficient observations for the receiver to compute an up to date solution. Since ground based commercial receivers are unable to propagate orbital dynamics, the receiver's velocity estimation becomes significantly

wrong within seconds, and the receiver must be reset with a cold or warm start.

For small satellites, there is an additional constraint on antenna field of view. Small satellites are often restricted in the number of antennas they are able to carry. This imposes additional restrictions on the attitude subsystem of micro and nanosatellites, as they must keep the antenna oriented to receive sufficient GPS signals throughout the mission. In many applications, such as Earth observing or communications missions, the satellite's attitude is already constrained to point instruments at specific primary targets. This implies that the satellite's attitude must point in two places at once, which is typically not possible, thus a compromise must be made. To further complicate the situation, the primary attitude targets may be frequently updating, necessitating large angle slew manoeuvres. If during these slews, the receiver is unable to keep uninterrupted communication with a sufficient number of GPS satellites, its position and velocity solution will become corrupted and a warm or cold start must be performed before new satellites will be acquired. Most commercial receivers will automatically perform a cold start after a sufficiently long blackout period, but the cold start requires upwards of 25minutes to complete [5,6]. Presented in this paper is an attitude controller that minimizes GPS dropouts due to large angle slews as validated by numerical simulations and experimental results from an on orbit GPS receiver.

CanX-4 and CanX-5 Satellites

The presented attitude controller was developed for the CanX-4 and CanX-5 satellites, which are two identical satellites being developed at the University of Toronto Institute for Aerospace Studies Space Flight Laboratory (UTIAS/SFL) which will demonstrate autonomous navigation and precision formation flying. Designed to make uses of the Generic Nanosatellite Bus (GNB), a flexible multi-mission platform also developed at UTIAS/SFL, the CanX-4 and CanX-5 satellites are cubic, 20cm a side and are less than 7kg in mass. Both satellites come equipped with a cold gas propulsion system, known as Canadian Nanosatellite Advanced Propulsion System (CNAPS), mounted along their X axis, and a GPS antenna mounted 90° away on their +Y face, as shown in Figure 1. Also onboard each satellite is a half-duplex inter satellite link (ISL) and a full suite of attitude sensor and actuators, including sun sensors, rate sensors, three axis magnetometer, magnetorquers and three orthogonally mounted reaction wheels. CanX-4 and CanX-5 will be three-axis-stabilized, achieving better than 1.5° of attitude determination while in Sunlight or Eclipse [9].

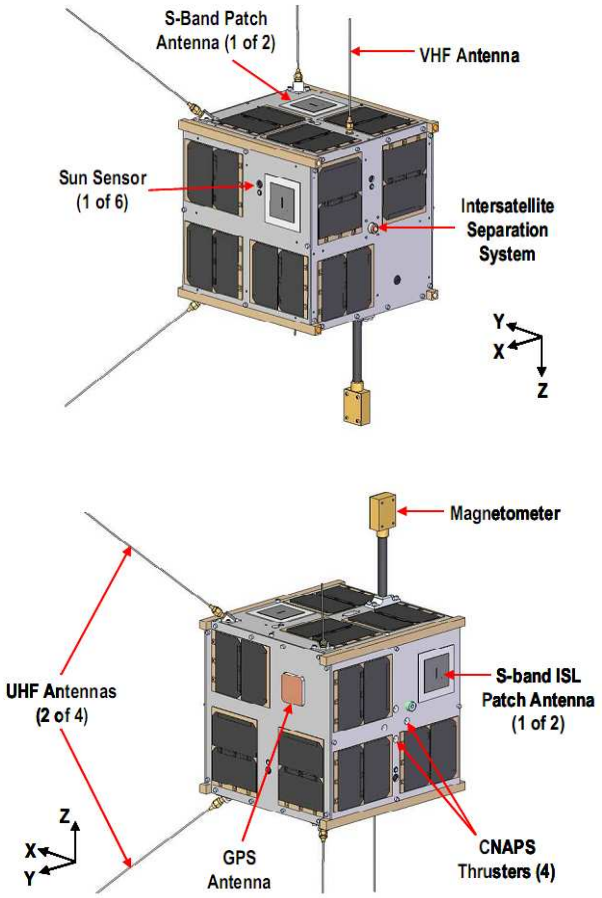

Figure 1: CanX-4 and CanX-5 [9]

Formation Flying Mission Overview

CanX-4 and CanX-5 will perform autonomous formation flying. Relative navigation will be performed by using differential GPS signals collected by both satellites. To perform the relative navigation both satellites must see a common set of GPS satellite from which to apply the differential navigation algorithms developed by the University of Calgary. The number of satellites required for fine navigation is four common GPS satellites, although there is a significant improvement once six satellites have been acquired. The formation flying algorithm has been developed to be robust to intermittent blackouts in GPS coverage. However, there is an increased cost in fuel and accuracy as a result of a momentary blackout in GPS coverage.

Once commissioning is complete and formation flying has commenced the mission will consist of several sequences, including fine and coarse station keeping as well as reconfiguration between various formations.

Throughout these sequences, commands will be issued from the onboard formation-flying algorithm with the next thrust direction. It is then up to the attitude controller to point the thrust axis in the required direction and hold it there until the thrust has finished and the next target is issued. The rate of the target updates, or the period of the formation-flying cycle, depends on the active mission sequence. During formation reconfiguration the formation-flying cycles can last several minutes each, but during fine formation control they have a 65s period [9]. Part of the formation-flying cycle is allocated for slewing the spacecraft before the thrust, as shown in Figure 2. In the 65s formation-flying cycle there is 50s for attitude reconfiguration, with a period of fine updates just prior to the thrust.

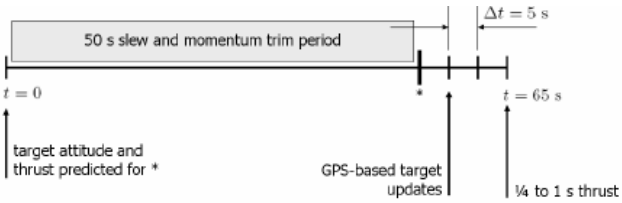

Figure 2: Fine Formation Control Cycle

GPS SATELLITE ACQUISITION

Of paramount interest in developing the attitude control strategy for CanX-4 and CanX-5 is the length of time it takes to acquire new GPS satellites as they come into the field of view of the antenna. This delay will drive the attitude manoeuvring strategy and is important in determining the effectiveness of the controller prior to launch.

GPS Constellation Overview

The Space component of the Global Positioning System consists of several operational and upcoming constellations of satellites including the US GPS, GLONASS and GALILEO [10]. The relative navigation to be used by CanX-4 and CanX-5 is has been developed to use signals from the US GPS constellation only. This constellation nominally includes 32 active satellites orbiting the Earth in 6 planes at an altitude of 30,000km [8].

CanX-2 On-Orbit GPS Acquisition

To confirm the behaviour of the commercial GPS receiver and to determine the time required to acquire new GPS satellites, a test campaign was performed with the CanX-2 satellite. CanX-2, launched on 28 April 2008, carries a modified NovAtel OEM4-G2L 12 channel receiver and AeroAntenna AT2775-103 aircraft antenna. This receiver is very similar in most respects to the modified OEMV-1G to be flown on the CanX-4 and CanX-5 satellites. The only major difference being that the OEMV-1G receives only L1 band compared to OEM4-G2L, which can receive L1 and L2.

It was desired to investigate the time it takes to acquire visible GPS satellites when the receiver has a complete solution calculated. Complicating this investigation are uncertainties in the antenna field of view and gain pattern, as well as the precise time of satellites rising over the horizon. What was desired was that the receiver attempt to acquire GPS satellites high in the antenna's field of view, starting at a controlled time to eliminate any uncertainties in synchronizing clocks to events. Two tests were developed and performed.

First, the receiver was cold started. Over the course of the cold start, the receiver attempts to acquire a lock on GPS satellites by searching through a band of Doppler shift frequencies. Once the receiver has a lock on four GPS satellite it is able to compute an accurate position and velocity solution. The channels not tracking these four satellites then begin to acquire additional GPS satellites using expected Doppler shift as estimated by the receiver. Acquiring a lock on GPS satellites with an estimated Doppler shift is much more rapid than the acquisition during the first phases of the cold start, without an estimate. The receiver uses an estimated Doppler shift when acquiring GPS satellites newly visible as the result of them rising over the horizon or an attitude slew. The time to acquire additional GPS satellites once the receiver had computed a solution was recorded. The second experiment attempted to restrict the search for additional GPS satellites until a specific time. The receiver was warm started using a method developed at the University of Calgary [6]. This warm start used six channels to attempt to acquire six GPS satellites, with the remaining six channels set to idle. After sufficient time for the receiver to compute a solution, all channels were activated and set to use the receiver's automatic search scripts. The time for each of the newly activated channels to a lock onto a GPS satellite was collected. Both of these experiments were performed twice and the times to acquire GPS satellites are listed in Table 1.

The reason for the acquisition delay comes from the receiver cycling through the different Doppler shift frequencies for each GPS satellites, attempting to acquire one for up to 5 seconds, depending on the receiver, before switching to another. The receiver is able to search through the potentially visible GPS satellites quickly if it has multiple channels open to search, but the search can take longer when only a few channels are available to lock onto GPS satellites. This means that the approximately 40 seconds upper bound

on the acquisition time, see Table 1, occurs only when there are many GPS satellites locked on, and additional satellites are not urgently required. In the more demanding case, when the direction of the antenna has changed significantly and new satellites are urgently needed, the acquisition time is typically shorter, as long as at least four satellites remained locked and the receiver is able to compute a solution.

Table 1: GPS Satellite Acquisition Times

	Experiment 1: Time Since Receiver Computed a Solution	Experiment 2: Time Since Channels Were Activated
Mean	17s	25s
Upper Bound	43s	41s
Lower Bound	2s	14s
Standard Deviation	16s	13s

For the numerical simulations discussed later, the acquisition delay time used was the mean time seen when activating idle channels. Both experiments are representative of nominal on orbit behaviour, however, the acquisition delay times when activating idle channels had a smaller spread, and thus a higher level of confidence compared to the cold start experiment.

GPS Acquisition Simulation

It is necessary to quantify the impact of the GPS acquisition delay on the number of GPS satellites a manoeuvring antenna can acquire. The scenario investigated was the worst reasonable spin geometry, which has the antenna's bore sight pointed along the local horizon and then spun at a constant rate about Nadir. In this configuration, Earth blocks half of the antenna's field of view and half a rotation will point the antenna's bore sight in the opposite direction, completely changing its field of view. To analyze the scenario, AGI's Satellite Tool Kit (STK) was used to propagate the orbits of the GPS constellation and of a test satellite, as illustrated in Figure 3.

STK is capable of calculating the access between various satellites and an antenna. The orbits of the GPS constellation and a test satellite, with the planned initial orbit of CanX-4 and CanX-5, were propagated within STK. A GPS antenna with an 80° half angle field of view was placed on the +Y face of the test satellite. The access times between each GPS satellite and this ideal GPS antenna were computed for several spin rates of the test satellite. To improve the statistical relevance of the simulation, the access times were computed for several orbits of the test satellite. To be conservative about the GPS satellite availability, one of the GPS satellites was removed from the simulation, as if it was experiencing an outage. The delay time was applied and the number of satellites locked on was tallied.

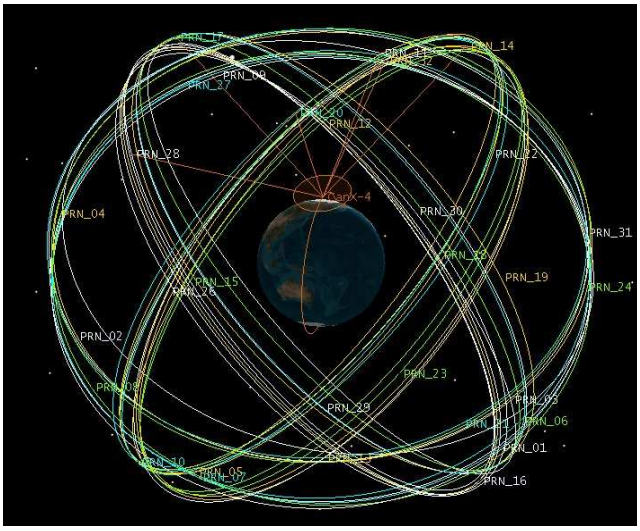

Figure 3: GPS Acquisition Simulation

Figure 4 shows the impact of various spin rates with a 25s delay in acquisition. As expected, a faster spin rate equates to GPS satellites remaining in the antenna's field of view for less time resulting in fewer satellites overcoming the 25s delay. Spin rates above 0.02rad/s results in the number of locked GPS satellites falling below four at times. Also of interest is the sensitivity of GPS coverage to the acquisition delay time. Shown in Figure 5 is a GPS coverage histogram for a 0.02rad/s spin rate with various delay times. As expected, the longer the delay time, the more the histogram shift towards fewer GPS satellite locked on. However, a change in the delay time of ±5s does not greatly affect the overall GPS coverage; the fewest satellites locked on remains to be four or higher.

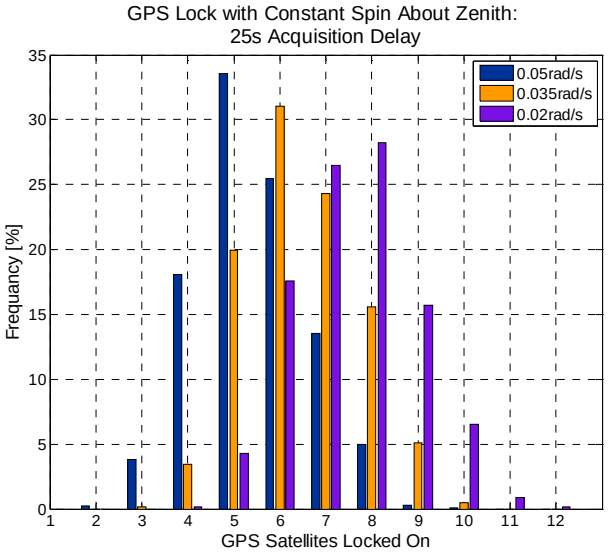

Figure 4: Effect of Spin Rate on GPS Lock

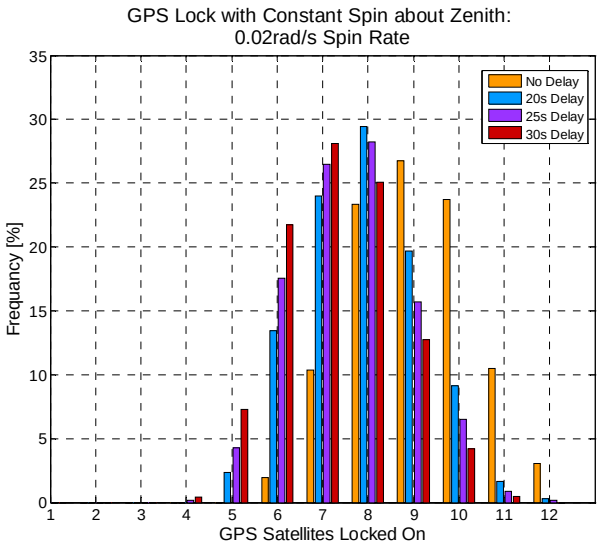

Figure 5: Effect of Delay Time on GPS Lock

ATTITUDE CONTROLLER

Controller Requirements

The attitude controller for the CanX-4 &-5 satellites must rapidly slew to updated thrust targets with a constraint to maximize the number of GPS satellites within the antenna's field of view and keep upwards of four specific GPS satellites locked on until the receiver has a chance to acquire additional GPS satellites. Table 2 summarizes the critical objectives and goals of the attitude subsystem for CanX-4 and CanX-5.

Table 2: Requirements for CanX-4 and CanX-5

Metric	Requirement
Thrust Axis Pointing (during thrust)	2° RMS
Thrust Axis Reposition Settling Time	50s
GPS Coverage Required	4 Satellites
GPS Coverage Desired	6 Satellites

Equations of Motion

The dynamics of a spinning body as expressed in the body frame is given by Euler's Equation [11].

$$\dot{\mathbf{h}} + \boldsymbol{\omega}^{\times}\mathbf{h} = \mathbf{G} \tag{1}$$

Where $\mathbf{h}$ is the total spacecraft angular momentum, $\dot{\mathbf{h}}$ is its time derivative, $\mathbf{G}$ is external disturbance torques and $\boldsymbol{\omega}^{\times}$ is the skew symmetric matrix of spacecraft angular velocity as given by

$$\boldsymbol{\omega}^{\times} = \begin{bmatrix} 0 & -\omega_z & \omega_y \\ \omega_z & 0 & -\omega_x \\ -\omega_y & \omega_x & 0 \end{bmatrix} \tag{2}$$

For a satellite with momentum or reaction wheels, equation (1) can be expanded into

$$\dot{\mathbf{h}}_{SC} + \dot{\mathbf{h}}_{w} + \boldsymbol{\omega}^{\times}(\mathbf{h}_{SC} + \mathbf{h}_{w}) = \mathbf{G} \tag{3}$$

where $\mathbf{h}_{SC}$ is the spacecraft's angular momentum and $\mathbf{h}_W$ is the angular momentum of the wheels. $\boldsymbol{\omega}$ remains the spacecraft's angular velocity. When using reaction wheels as attitude control actuators, $\dot{\mathbf{h}}_W$ is commanded to control $\dot{\mathbf{h}}_{SC}$ and counter the effects of the disturbances and the nonlinear term.

Quaternion Control

The use of quaternions for attitude parameterization is a well-established practice [11,12]. Quaternions have no singularities, which makes their use preferred in large angle slews, where it is difficult to ensure the attitude will stay clear of any singularity points. Quaternions describe rotations with an axis of rotation and an angle about it, as shown.

$$q_{ei} = a_i \sin(\phi/2) \tag{4.a}$$

$$q_{e4} = \cos(\phi/2) \tag{4.b}$$

$$q_1^2 + q_2^2 + q_3^2 + q_4^2 = 1 \tag{4.c}$$

where *i=1, 2,* or *3* and $\boldsymbol{a}$ is the Euler axis of rotation with ϕ being the angle of rotation about that axis. The error quaternion is defined as the required rotation between the current, $\mathbf{q_S}$, and target state, $\mathbf{q}_T$, and follows the typical quaternion multiplication laws as

$$\mathbf{q}_E = \mathbf{q}_T\mathbf{q}_S = \begin{bmatrix} q_{T4} & q_{T3} & -q_{T2} & q_{T1} \\ -q_{T3} & q_{T4} & q_{T1} & q_{T2} \\ q_{T2} & -q_{T1} & q_{T4} & q_{T3} \\ -q_{T1} & -q_{T2} & -q_{T3} & q_{T4} \end{bmatrix} \begin{bmatrix} q_{S1} \\ q_{S2} \\ q_{S3} \\ q_{S4} \end{bmatrix} \tag{5}$$

Time Optimal Control

Due to the need to perform rapid large angle slews, the use of a time optimal control approach is warranted. Extensive work has been done on time optimal attitude control, with both single axis [13] and three-axis [14] slews having been considered. The solution to the time optimal problem is a bang-bang style controller which applies maximum control effort towards the intended target, and then applies the opposite control effort to arrest the motion once the velocity is sufficiently high compared to the remaining distance to target. In the single axis case, ignoring the nonlinear terms of (1), the sign of the control effort is switched once the angle of

rotation to the target is less than the estimated angular distance traveled before the maximum control force can arrest the current velocity. The sign of the control effort is given by

$$T = \phi + \frac{|\omega|}{2U}\omega \tag{6}$$

where T is the sign of the control command, ϕ is the angle of rotation for the current position to the target, and U is the maximum acceleration, given by the maximum actuator torque over the moment of inertia.

$$U = \frac{\tau_{\max}}{I} \tag{7}$$

where $\tau_{\max}$ is the maximum torque that the actuators can provide. While the time optimal control ensures the minimum time to slew under perfect conditions, there will inevitably be oscillations around the zero point due to disturbances and uncertainties in the moment of inertia. To add a measure of robustness and to smooth the control performance near the target attitude, a proportional and derivative (PD) control law is implemented as suggested in [13]. The PD control law using quaternion feedback is given by [13]

$$T_i = 2K_{pi}q_{ei}q_{e4} + K_{di}\omega_i \tag{8}$$

where i =1, 2 and 3 and K_p and K_d are computed in the standard way

$$K_{pi} = I_{ii}\omega_n^2 \tag{9.a}$$

$$K_{di} = 2I_{ii}\xi\omega_n \tag{9.b}$$

where ω_n is the natural frequency of the controller's response and ξ is the damping coefficient. The PD control law is used if the actuator will not be saturated by the derivative portion of the control law. When the target attitude is updated, the proportional term in the control law will quickly saturate the actuator due to the large error signal. As the angular velocity increases, the controller switches to the time optimal logic. While operating in the time optimal mode, (6) determines the sign of the control effort, which is then set to the maximum actuator output. After the satellite's angular rate reduces to the point that the PD control can take over without saturating the actuators, the controller transitions back into the PD control logic to provide smooth control near the target. The controller, outlined in Figure 6, provides smooth and time optimal control, where the $\text{sign}[T_{\max}, T]$ function is used to scale the actuator command, T_C, to the maximum actuator output, $T_{\max}$, while preserving the sign of the controller output, T.

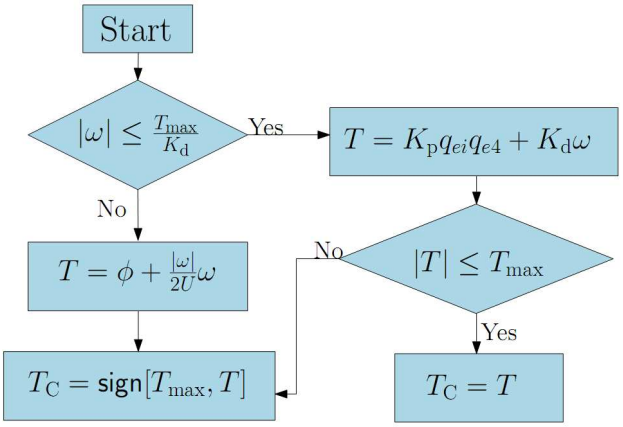

Figure 6: Time Optimal Controller

To ensure the controller always produces a critically damped response, a margin, *P*, can be applied to the satellite's angular acceleration as.

$$U = \frac{\tau_{\max}}{I}(1-P) \tag{11}$$

The effect of this margin is to trigger the actuation reversal earlier. This ensures that even in the presence of disturbances and uncertainties in the moment of inertia, the angular velocity approaches zero faster than the position approaches the target, leaving more distance for the PD controller to traverse once it takes over. The obvious cost to this is a longer slew time, but the cost of over shooting the target results in even longer settling times and sweeping the GPS antenna further reducing GPS coverage.

The control laws above work well only in a single axis case with the nonlinear terms of (1) neglected. However, a slew about a single axis is rarely required, and the presence of angular momentum stored in reaction wheels make the nonlinear terms very significant. The use of time optimal controllers for 3-axis slew has been investigated, and several solutions exist that give a performance improvement by taking advantage of motion in other axes [14]. These controllers move other axis off target for a portion of the slew, which is often unacceptable when tracking the secondary targets, like the GPS constellation. Instead, a feed forward term can be added to the controller to cancel the majority of the effects of the nonlinear terms in (3), linearizing the dynamics. The feed forward torque is given by

$$\mathbf{T_{ff}} = -\boldsymbol{\omega}^{\times}\left(\mathbf{h}_{SC} + \mathbf{h}_{W}\right) \tag{12}$$

The command to the reaction wheels is the sum of the feed forward and feedback terms.

$$\mathbf{T_W} = \mathbf{T_C} + \mathbf{T_{ff}} \tag{13}$$

The time optimal controller often attempts to saturate the reaction wheel's torque output. The addition of the feed forward control would be ineffective if the actuators are already saturated. It is necessary to limit the time optimal actuator commands to a level below the actual actuator saturation point to allow the feed forward term sufficient control authority to eliminate the effect of the gyric stiffness of the reaction wheels.

Roll About Thrust Axis

The attitude targets coming out of the formation flying script pertain only to the direction of the thrust axis, and do not constrain the roll about the thrust axis. In order to maximize GPS coverage, it is important to point the GPS antenna, mounted perpendicular to the thrust axis, towards the greatest concentration of GPS satellites. Since the Earth blocks GPS signals, it is preferred to point the GPS antenna away from the Earth, towards Zenith.

The target attitude rotation between the satellite's body frame and the inertial frame is generated as an Euler axis rotation derived from the primary target, in this case the thrust target. To generate a target rotation matrix, we assume that the inertial frame and the body frame are aligned; we can then define an Euler axis rotation that transforms the body frame such that it aligns with the target. The Euler axis for this rotation is perpendicular to desired thrust direction in the inertial frame and the thrust axis, computed as the cross product

$$\mathbf{a} = \mathbf{x}_i \times \mathbf{T}_i \tag{14}$$

where $\mathbf{x}_i$ is the non rotated thruster axis in the inertial frame, in this case the X direction, [1 0 0], $\mathbf{T}_i$ is the thrust target in the inertial frame, and $\mathbf{a}$ is the Euler axis. The required rotation about this Euler axis is computed from the angle between the non rotated thruster axis and the target thrust axis, computed by

$$\theta = \arccos(\mathbf{x}_i \bullet \mathbf{T}_i) \tag{15}$$

The corresponding rotation matrix is given by

$$\mathbf{C_{bi,u}} = \cos(\theta)\mathbf{1} + (1-\cos(\theta))\mathbf{a}\mathbf{a}^{\mathbf{T}} - \sin(\theta)\mathbf{a}^{\times} \tag{16}$$

where $\mathbf{C_{bi,u}}$ is the unconstrained target body to inertial frame rotation matrix and $\mathbf{a}^{\times}$ is the skew symmetric matrix given by

$$\mathbf{a}^{\times} = \begin{bmatrix} 0 & -a_3 & a_2 \\ a_3 & 0 & -a_1 \\ -a_2 & a_1 & 0 \end{bmatrix} \tag{17}$$

This target rotation is considered unconstrained as it has an arbitrary, or unconstrained, roll about the thrust axis. It is possible to modify this unconstrained target rotation to align the GPS antenna, which is mounted on the body Y face, with Zenith. To compute the desired roll about the thrust axis, the satellite's position in the unconstrained target frame must be known. The position in the inertial frame is typically available from an onboard orbit propagator, and can be transformed in to the target body frame with the rotation matrix computed in (16).

$$\mathbf{r_b} = \mathbf{C_{bi,U}}\mathbf{r_i} \tag{18}$$

The magnitude of the rotation is equal to the angle between Zenith and the body Y axis in the unconstrained target frame projected on to the plane normal to the constrained axis, in this case the body X axis. The projected angle is given by

$$\alpha = \arctan\left(\frac{r_{b,3}}{r_{b,2}}\right) \tag{19}$$

where $r_{b,3}$ and $r_{b,2}$ are the Z and Y components of the satellite's position vector in the unconstrained target frame. The rotation matrix between the unconstrained target frame and the constrained target frame is given by a rotation about the X or 1 axis

$$\mathbf{C_1} = \begin{bmatrix} 1 & 0 & 0 \\ 0 & \cos(\alpha) & \sin(\alpha) \\ 0 & -\sin(\alpha) & \cos(\alpha) \end{bmatrix} \tag{20}$$

With the roll about the thrust axis computed the final target rotation matrix is given as the product of the rotations computed above, as

$$\mathbf{C_{bi}} = \mathbf{C_1}\mathbf{C_{bi,u}} \tag{21}$$

Roll Limited Time Optimal Control

GPS coverage is based on more than just keeping the antenna pointed as near Zenith as possible. The delay

in acquiring new GPS satellites means that rapid slews will negatively impact the number of GPS satellites locked on. It is required to point the thrust axis in the desired direction with the utmost speed, and as such, there is no flexibility in reducing the thrust axis slew times. However, any roll about the thrust axis is performed primarily to improve GPS coverage. This gives the freedom to perform the roll manoeuvre at a set rate to accommodate the GPS acquisition delay. It was shown previously that with the demonstrated 25s delay in acquiring new GPS satellites, spin rates of 0.035rad/s and above would often limit the GPS coverage to less than four GPS satellites locked on at a time. To improve the GPS coverage the roll rate about the thrust axis should be limited to below 0.035rad/s.

The time optimal controller is unchanged from what was developed above, with the addition of limiting the angular velocity about the thrust axis. Shown in Figure 7 is the schematic of the time optimal controller for the body X-axis, with the additional roll limiting logic. The other two axes remain the same as before. If the magnitude of roll angular velocity is less than the prescribed limit, $\boldsymbol{\omega}_{\text{ref}}$, the controller behaves identically to the time optimal controller described in Figure 6. Once roll velocity approaches the desired limit the controller switches to a pure derivative control, tracking the reference angular velocity. As the position approaches the desired location, the controller switches back to a PD control law once the controller detects that the PD control law would further slow the limited roll velocity.

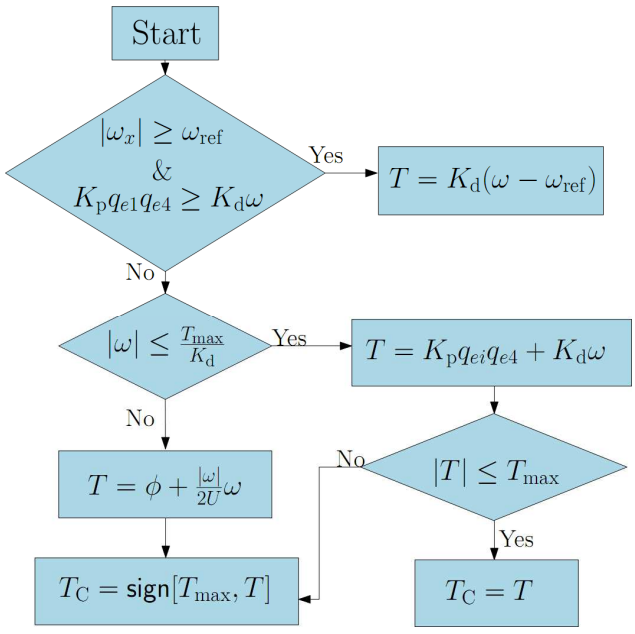

Figure 7: Time Optimal Controller-Roll Limited

SIMULATION RESULTS

Numerical simulations were performed to assess the performance of the time optimal controller with and without applying a limit on the roll rate about the thrust axis. The formation flying script was ran for a three orbit simulated mission profile including an orbit of reconfiguration and orbit of fine formation control, 65s formation-flying cycle, and an orbit of coarse formation control, 300s formation-flying cycle. The thrust targets from the formation flying simulation were used in numerical attitude simulation, which was performed twice, once with the roll rate about the thrust axis unrestricted, and once again with the roll rate limited to 0.025rad/s. The attitude simulation included noise on the attitude position and velocity equal to what is expected on orbit.

Over the three simulated orbits, the attitude controller was forced to perform over one hundred large angle manoeuvres. The times required to settle thrust axis within 2° of the target are plotted against the magnitude of the attitude manoeuvre in Figure 8. As expected, there is a relation between the slew magnitude and the time required to reorient the spacecraft; with larger slews requiring more time. However, the attitude controller is able to slew the satellite within the required 50s for all attempted slews. It is important to note that adding the roll rate limit of 0.025rad/s does not significantly affect the settling time of the thrust axis. There are a few manoeuvres, where the initial and final thrust axes are near Zenith, which are slower with the limited roll rate, since the angular path is longer as a result of the limited roll rate. These manoeuvres are all around 45° in magnitude, and are still within the 50s settling time requirement. It was found that limiting the roll rate beyond 0.025rad/s can have a more pronounced and undesirable impact of the settling times.

The attitude at each time step of the simulation was fed into STK to compute the GPS coverage. To make the simulation a more conservative representation a GPS satellite was excluded to simulate a satellite outage, leaving a constellation of only 31 satellites. The 25s delay was applied, as described previously, to the fine formation-flying mode, with a formation-flying cycle period of 65s, which is the limiting case for GPS tracking. The histogram of the GPS coverage for one orbit of fine formation flying is plotted in Figure 9 and summarized in Table 3. By adjusting the roll about the thrust axis in order to direct the GPS antenna as close as possible to Zenith results in GPS coverage that includes predominantly four or more satellites. However, there are still several dropouts when three or fewer satellites locked on. Limiting the roll rate reduced the impact of

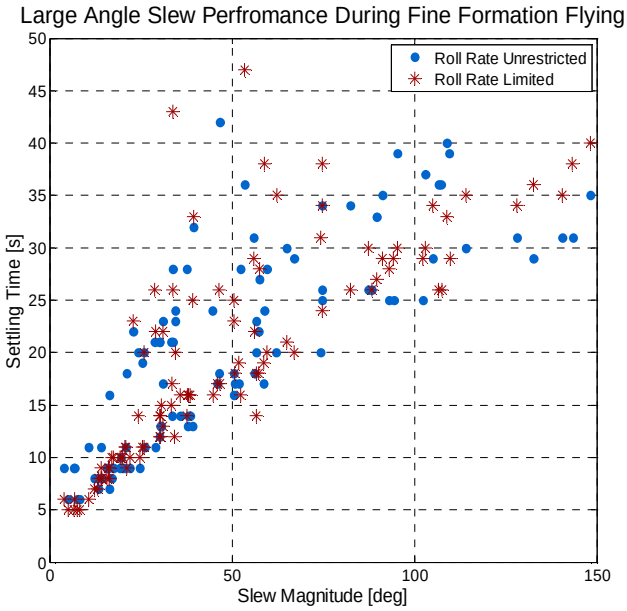

Figure 8: Attitude Settling Times

the delay associated with locking on to newly visible GPS satellites. This improves the GPS coverage, effectively shifting the centroid of the distribution in Figure 9. The number of dropout events per orbit is cut to a quarter by instigating the roll rate limitation of 0.025rad/s. All of the dropout events with the roll rate limited were less than 1minute in length.

Table 3: GPS Lock on During Fine Formation Flying

GPS Satellites	Roll Rate Unrestricted	Roll Rate Restricted to 0.025rad/s
Dropouts (<4)	12	3
Coverage with 4+	97.6%	99.4%
Coverage with 6+	84.7%	88.3%

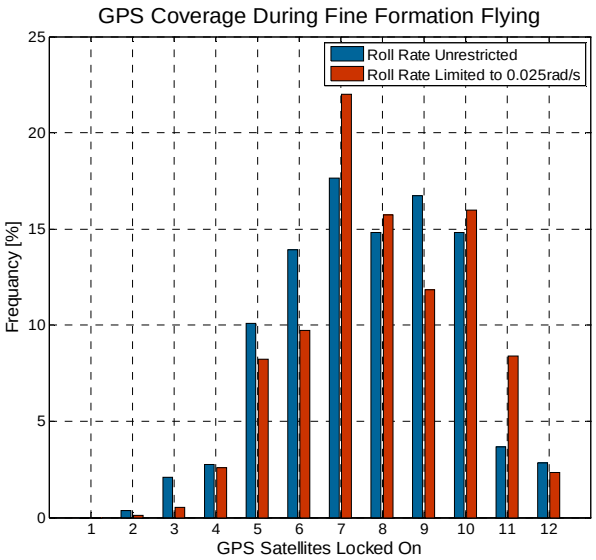

Figure 9: GPS Lock on During Fine Formation Flying

CONCLUSION

The ability to maintain GPS coverage while performing aggressive attitude manoeuvres presents a challenge for small satellites with a limited GPS antenna field of view. The problem is two fold, to keep the GPS antenna towards the majority of the GPS satellites and to slow the slew rate of the antenna to accommodate the delay in acquiring new GPS satellites. The solution to these problems could be applied to the tracking of secondary targets other than the GPS constellation, such as communication relay satellites and ground stations.

Based on on-orbit experiments with the CanX-2 satellite, the delay in acquiring a lock on a newly visible GPS satellite with a commercial OEM4 receiver, when an accurate solution has been computed, was determined to be approximately 25s. The delay is shorter when more channels are available for searching, such as when the number of locked on satellites is low.

The attitude required to point a single axis of the satellite at a target has the freedom to roll about that axis. The initial target attitude can be transformed to orient a perpendicular axis towards a secondary target. Depending on the position of the secondary target relative to the primary target, it is not always possible to track the secondary target perfectly. However, the secondary target will be tracked within 90°. This approach for GPS tracking while performing rapid slews will result in maintaining a lock on four or more satellites more than 95% of the time, according to numerical simulations. This still leads to frequent though short-lived dropouts in GPS coverage, with three or less satellites locked on, the receiver cannot calculate a solution. With a commercial receiver in an orbital environment, a dropout of almost any length could result in the receiver becoming lost, necessitating a lengthy warm or cold restart.

Many of the dropouts occur when GPS satellite are visible, but not yet locked onto the receiver. To reduce the impact of this, a limit was applied to the angular velocity about the degree of freedom left by the primary attitude target. Making this limit arbitrarily restrictive had a significant and unacceptable impact on the settling time of slewing to a primary attitude target. However, a limit of 0.025rad/s was shown to have little to no effect on the settling time and did significantly improve the GPS coverage. A limit of 0.025rad/s reduced the number of dropouts to three in the simulated orbit, a quarter of what they were without the limit.

Some dropouts are inevitable due to the unevenness of the GPS constellation and with the Earth blocking a large portion of the sky with some primary targets.

However, simulations predict the number of dropouts with the presented attitude controller to be three per orbit, with large angle slews of the primary target required every 65s. While work to reduce this number further is ongoing, it is likely that this is near the ideal case, and steps to make the mission robust to GPS dropouts of this frequency will be investigated.

ACKNOWLEDGMENTS

The authors wish to acknowledge the ongoing contributions of all the CanX-4 and CanX-5 student team: Scott Armitage, Laura Bradbury, Jennifer Elliott, Micheal Ligori, Jakob Liftshits, Neils Roth, and Jakub Urbanek. In addition, the authors would like to acknowledge the mentorship received from the SFL staff: Mihail Barbu, Grant Bonin, Cordell Grant, Stephen Mauthe and Karan Sarda. A special thank you to Jakub Urbanek and Karan Sarda for operating CanX-2 during the test campaign. Finally the authors would like to acknowledge the research contributions of Dr. Elizabeth Cannon at the University of Calgary and Dr. Christopher Damaren at the University of Toronto. The UTIAS Space Flight Laboratory gratefully acknowledges the following sponsors of the CanX program:

- Canadian Space Agency
- Defense Research and Development Canada (Ottawa)
- Natural Sciences and Engineering Research Council of Canada (NSERC)
- Ontario Centers of Excellence (OCE)
- MDA Space Missions
- Routes AstroEngineering
- Sinclair Interplanetary

In addition, the following organizations have made valuable donations to the program: AeroAntenna Technology Inc. – Agilent Technologies – @lliance Technologies – Altera – Alstom – Altium – Analytical Graphics Inc. – Ansoft ARC International – ATI – Autodesk – Cadence – CMC Electronics – EDS – E. Jordan Brookes – Emcore – Encad – Honeywell – Micrografx – National Instruments – Natural Resources Canada – NovAtel Inc. – NRCan – Raymond EMC – Rogers Corporation – Stanford University – Texas Instruments – The MathWorks – Wind River.

REFERENCES

1. Montenbruck, O., Markgraf, M., et al. "Autonomous and Precise Navigation of the PROBA-2 Spacecraft." *AIAA Astrodynamics Specialist Conference*, Honolulu, 18-21 Aug. 2008.
2. Wermuth, M., Hauschild, A., et al. "TerraSAR-X Rapid and Precise Orbit Determination." *21st International Symposium on Space Flight Dynamics*, Toulouse, 28 Sept-2 Oct, 2009.
3. van Mierlo, M., Yoshihara, K., et al. "Earth Observation Using Japanese/Canadian Formation Flying Nanosatellites." in *Small Satellite Missions for Earth Observation: New Developments and Trends*. Sandau, R., Röser, H., Valenzuela, A. Ed. Springer, 2010 pp. 165-174.
4. Montenbruck, O., Kahle, R., et al. "Navigation and Control of the TanDEM-X Formation." *Journal of the Astronautical Sciences.* Vol 56, No 3, July-Sept 2008, pp. 341-357.
5. Leung, S. Y. F., Montenburck, O. and Bruninga, B., "Hot Start of GPS Receivers for LEO Microsatellites," in *1st ESA Workshop on Satellite Navigation User Equipment Technologies NAVITEC*, Noordwijk, Dec 2001.
6. Kahr, E., "Operatin the CanX-2 GPS Receiver in Orbit," *Department of Geomatics Engineering, University of Calgary, Schulich School of Engineering.*
7. Cecchini, J., "Next Generation GPS Aided Space Navigation Systems," *IEEE AESS Systems Magazine*, December 2002.
8. NovAtel OEM4 Family of Receivers Users Manual. Rev 12.
9. Eagleson, S., Sarda, K., Philip, A., Grzymisch, J., "Attitude Determination and Control: CanX-4/-5 Critical Design Review," *SFL-Internal Document.* 30 March 2007.
10. EVP Europe, "A Beginners Guide to GNSS in Europe." *International Federation of Air Traffic Controllers' Association.* Aug. 1999.
11. Hughes, P., Spacecraft Attitude Dynamics, Dover Publications, 1986.
12. Wie, B., Weiss, H., and Arpostathis, A., "Quaternion Feedback Regulator for Spacecraft Eigenaxis Rotations," *Journal of Guidance, Control, and Dynamics*, Vol 12, No 3, May-June 1989, pp. 375-380.
13. Sidi, Marcel J., Spacecraft Dynamics and Control, Cambridge University Press, 1997.
14. Bilimoria, K., and Wie, B., "Time-Optimal Three-Axis Reorientation of a Rigid Spacecraft," *Journal of Guidance, Control, and Dynamics*, Vol 16, No 3, May-June 1993, pp. 446-452.